



The following Communications have been judged by at least two referees to be “very important papers” and will be published online at www.angewandte.org soon:

M. Barsukova-Stuckart, N. V. Izarova, G. B. Jameson, V. Ramachandran, Z. Wang, J. v. Tol, N. S. Dalal,* R. N. Biboum, B. Keita, L. Nadjio, U. Kortz*

The Dicopper(II)-Containing 22-Palladate(II)

$[\text{Cu}^{\text{II}}_2\text{Pd}^{\text{II}}_{22}\text{P}^{\text{V}}_{12}\text{O}_{60}(\text{OH})_8]^{20-}$

H. Ishikawa, M. Honma, Y. Hayashi*

One-Pot Synthesis of a DPP4 Inhibitor by a Four-Component Coupling Reaction Mediated by Diphenylprolinol Silyl Ether

A. V. Zabula, S. N. Spisak, A. S. Filatov, A. Y. Rogachev, M. A. Petrukhina*

Strain-Releasing Trap for Highly Reactive Electrophiles: Structural Characterization of Bowl-Shaped Arenium Carbocations

H. C. S. Chan, J. Kendrick, F. J. J. Leusen*

The Tale of Molecule VI, a Benchmark Sulfonimide for Crystal-Structure Prediction: Are Its Polymorphs Predictable?

F. E. Zilly, J. P. Acevedo, W. Augustyniak, A. Deege, U. W. Häusig, M. T. Reetz*

Tuning a P450 Enzyme for Methane Oxidation

A. Nagy, J. Fulara, I. Garkusha, J. P. Maier*

On the Benzylum/Tropylium-Ion Dichotomy: Electronic Absorption Spectra in Neon Matrices

R. P. Sonawane, V. Jheengut, C. Rabalakos, R. Larouche-Gauthier, H. K. Scott, V. K. Aggarwal*

Enantioselective Construction of Quaternary Stereogenic Centers from Tertiary Boronic Esters: Methodology and Applications

X. Lang, H. Ji, C. Chen, W. Ma,* J. Zhao*

Selective Formation of Imines by Aerobic Photocatalytic Oxidation of Amines on TiO_2

G. Kummerlöwe, B. Crone, M. Kretschmer, S. F. Kirsch,* B. Luy*
Residual Dipolar Couplings as a Powerful Tool for Constitutional Analysis: Revealing the Unexpected Formation of Tricyclic Compounds



“When I was eighteen I wanted to be a professional baseball player.
The biggest challenge facing scientists is to convince the funding agencies that what they do is meaningful ...”
This and more about Steven P. Nolan can be found on page 2212.

Author Profile

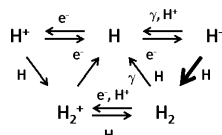
Steven P. Nolan _____ 2212

Stable Radicals

Robin G. Hicks

Books

reviewed by J. C. Walton _____ 2213



A star is born: The formation of H_2 was crucial to the generation of the first stars and possibly the first galaxies. The rate of H_2 generation by associative detachment (thick arrow in the scheme of the reactions of hydrogen in the early universe) has now been determined experimentally and may provide a more detailed understanding of the birth of the first stars.

Highlights

Astrochemistry

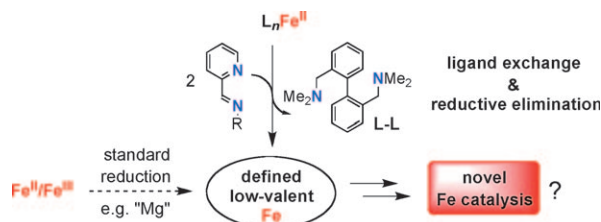
S. Schlemmer* _____ 2214–2215

H_2 Generation in the Early Universe
Governs the Formation of the First Stars

Iron Catalysis

O. García Mancheño* — 2216–2218

New Trends towards Well-Defined Low-Valent Iron Catalysts



Less is more: This Highlight describes a simple new procedure to access well-defined formal low-valent iron complexes by ligand exchange and reductive elimi-

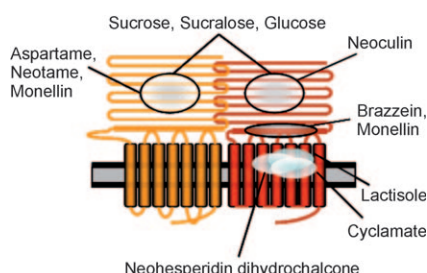
nation (see scheme). This method offers a good starting point for the further development of iron catalysts.

Reviews

Chemistry of Taste

M. Behrens, W. Meyerhof, C. Hellfrisch, T. Hofmann* — 2220–2242

Sweet and Umami Taste: Natural Products, Their Chemosensory Targets, and Beyond

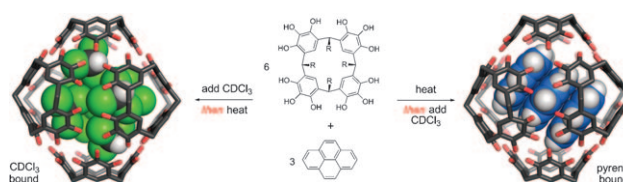


A question of taste: Much of our appreciation of food is due to the excitement of the “sweet” and “umami” taste. This Review gives a survey of compounds that elicit the sweet or umami taste. It will highlight the activation of the taste receptors and signal transduction, which induces neural activity and is conveyed to the cerebral cortex to represent the taste quality (the picture shows a binding site of a sweet taste receptor).

Communications

Supramolecular Chemistry

M. Kvasnica, J. C. Chapin, B. W. Purse* — 2244–2248



Efficient Loading and Kinetic Trapping of Hexameric Pyrogallolarene Capsules in Solution

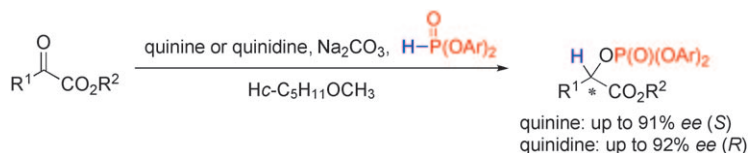
Solvent matters: By carrying out the assembly of pyrogallolarene hexamers under thermal conditions in the absence of solvent, highly efficient loading of guest

molecules to produce kinetically trapped assemblies was achieved. Such products are not formed when the solvents are present (see schematic).

For the USA and Canada: ANGEWANDTE CHEMIE International Edition (ISSN 1433-7851) is published weekly by Wiley-VCH, PO Box 191161, 69451 Weinheim, Germany. Air freight and mailing in the USA by Publications Expediting Inc., 200 Meacham Ave., Elmont, NY 11003. Periodicals

postage paid at Jamaica, NY 11431. US POSTMASTER: send address changes to *Angewandte Chemie*, Journal Customer Services, John Wiley & Sons Inc., 350 Main St., Malden, MA 02148-5020. Annual subscription price for institutions: US\$ 9442/8583 (valid for print and electronic / print or electronic delivery); for

individuals who are personal members of a national chemical society prices are available on request. Postage and handling charges included. All prices are subject to local VAT/sales tax.



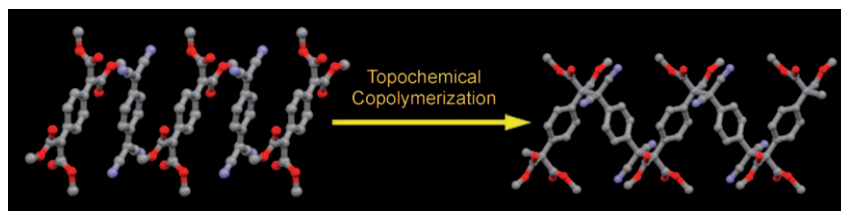
Phosphonates go chiral: The organocatalytic enantioselective reaction of α -ketoesters with phosphites using cinchona alkaloids and Na_2CO_3 has afforded α -phosphonyloxy esters with high enan-

tiomericities (see scheme). This process allows the formation of both enantiomers of the product. A catalyst loading of as low as 2 mol % does not result in a significant decrease of the enantioselectivity.

Asymmetric Synthesis

M. Hayashi, S. Nakamura* 2249–2252

Catalytic Enantioselective Protonation of α -Oxygenated Ester Enolates Prepared through Phospha-Brook Rearrangement



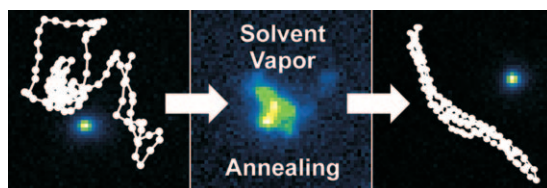
From single crystal to single crystal: A crystalline charge-transfer complex of the title compounds underwent topochemical polymerization through a radical mechanism under UV irradiation or upon heat-

ing. This *cis*-specific solid-state copolymerization of the substituted quinodimethanes required the alternating monomers in the cocrystal to tilt (see picture).

Solid-State Photopolymerization

T. Itoh,* T. Suzuki, T. Uno, M. Kubo, N. Tohnai, M. Miyata 2253–2256

Cis-Specific Topochemical Polymerization: Alternating Copolymerization of 7,7,8,8-Tetrakis-(methoxycarbonyl)quinodimethane with 7,7,8,8-Tetracyanoquinodimethane in the Solid State



An inside job: By using single-molecule spectroscopy (SMS) several effects of solvent vapor induced annealing (SVA) were studied directly on single conjugated polymers, e.g.: SVA-induced translocations, folding/unfolding dynamics, and

changes in the morphological order. It is shown that single chains can be trapped by spin-coating in a disordered conformation and subsequent SVA leads to an equilibrated, highly ordered conformation (see picture).

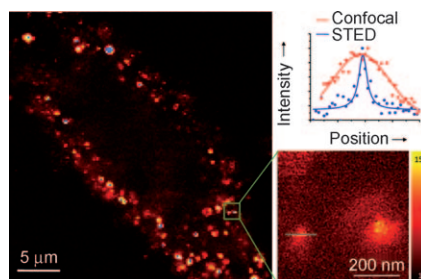
Single-Molecule Studies

J. Vogelsang,* J. Brazard, T. Adachi, J. C. Bolinger, P. F. Barbara 2257–2261

Watching the Annealing Process One Polymer Chain at a Time



A bunch of loners: Fluorescent nanodiamonds (FNDs) noncovalently conjugated with bovine serum albumin (BSA) or α -lactalbumin exhibited good dispersibility in a buffer with only minor or no agglomeration. They are useful as photostable fluorescent markers in cells for super-resolution imaging by STED (see confocal fluorescence image of an FND-labeled cell (left) and STED image of single BSA-conjugated FNDs (right)).



Biolabeling

Y.-K. Tzeng, O. Faklaris, B.-M. Chang, Y. Kuo, J.-H. Hsu, H.-C. Chang* 2262–2265

Superresolution Imaging of Albumin-Conjugated Fluorescent Nanodiamonds in Cells by Stimulated Emission Depletion

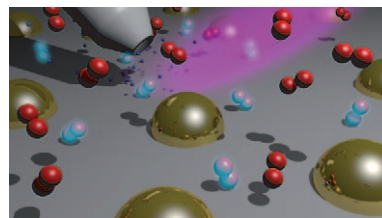


Charge Transfer

S. Porsgaard, P. Jiang, F. Borondics,
S. Wendt, Z. Liu, H. Bluhm,
F. Besenbacher,
M. Salmeron* ————— 2266 – 2269

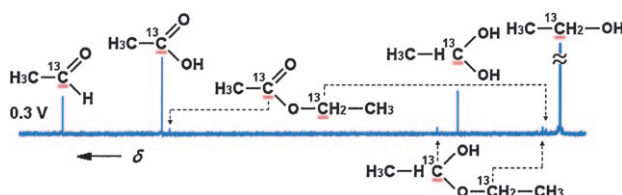
Charge State of Gold Nanoparticles
Supported on Titania under Oxygen
Pressure

Reversible band bending induced by adsorption of molecular oxygen on $\text{TiO}_2(110)$ was revealed by studying the charge state of TiO_2 -supported Au nanoparticles under O_2 pressure by X-ray photoelectron spectroscopy (see picture). This result is important for correct assignment of charge-transfer phenomena on catalysts in general, and with regard to the high catalytic activity of Au/ TiO_2 catalysts in numerous reactions, including CO oxidation.



Fuel Cells

I. Kim, O. H. Han,* S. A. Chae, Y. Paik,
S.-H. Kwon, K.-S. Lee, Y.-E. Sung,
H. Kim ————— 2270 – 2274



Catalytic Reactions in Direct Ethanol Fuel Cells

Different anode catalysts (Pt/C, PtRu/C, Pt₃Sn/C) and operating potentials lead to different product distributions in the anode exhaust of direct ethanol fuel cells, as shown by liquid-state ^{13}C NMR spectroscopy (see typical spectrum). Addition

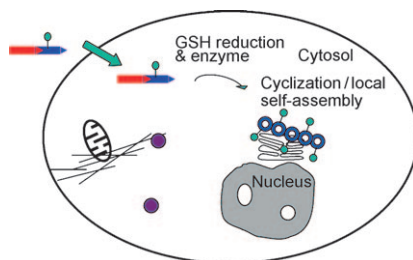
of Ru or Sn to Pt/C increases current density, mainly because of enhanced acetic acid production, and the potential dependences of products give clues to reaction pathways of ethanol electro-oxidation.

Macrocyclization in Cells

D. Ye, G. Liang, M. L. Ma,
J. Rao* ————— 2275 – 2279



Controlling Intracellular Macrocyclization for the Imaging of Protease Activity



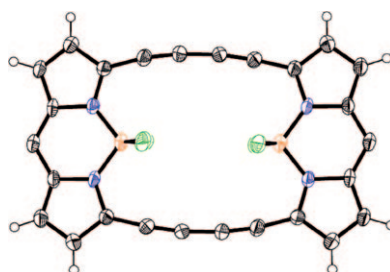
Reporters on the ground: An intramolecular macrocyclization reaction took place highly efficiently in live cells under the control of a specific enzyme and reduction by glutathione (GSH; see picture). Macrocyclic products (represented as blue rings) synthesized in cells self-assembled into nanoparticles aggregated and retained at the site near the enzyme location to report local proteolytic activity in live cells.

Antiaromaticity

T. Sakida, S. Yamaguchi,
H. Shinokubo* ————— 2280 – 2283

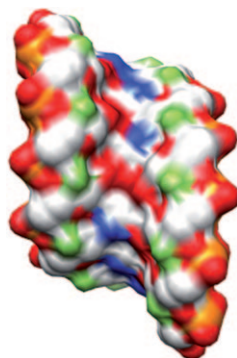


Metal-Mediated Synthesis of Antiaromatic Porphyrinoids from a BODIPY Precursor



Metallic route to antiaromaticity: The synthesis of a butadiyne-bridged cyclic BODIPY dimer (see structure; C white, B orange, N blue, F green) and trimer was achieved through Pd-catalyzed Stille coupling and Cu-mediated Glaser-type coupling. These cyclic BODIPYs were found to be stable 24π - and 36π -antiaromatic porphyrinoids with planar conformations, and their structures, electronic states, and reactivity were explored.

With little or no negative impact on the activity of small interfering RNAs (siRNAs), regardless of the number of modifications or the positions within the strand, the 2'-deoxy-2'-fluoro (2'-F) modification is unique. Furthermore, the 2'-F-modified siRNA (see crystal structure) was thermodynamically more stable and more nuclease-resistant than the parent siRNA, and produced no immunostimulatory response.



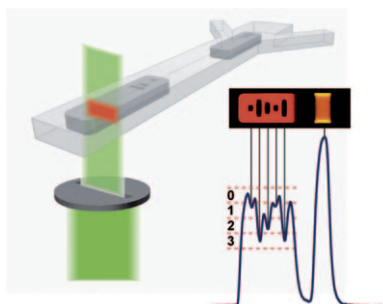
RNA Interference

M. Manoharan,* A. Akinc, R. K. Pandey, J. Qin, P. Hadwiger, M. John, K. Mills, K. Charisse, M. A. Maier, L. Nechev, E. M. Greene, P. S. Pallan, E. Rozners, K. G. Rajeev, M. Egli* — 2284–2288

Unique Gene-Silencing and Structural Properties of 2'-Fluoro-Modified siRNAs



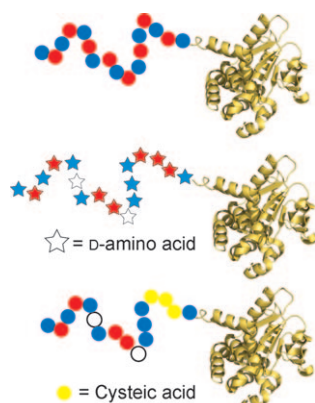
Sensitive, flexible, and rapid: A post-hybridization labeling scheme was combined with a high-throughput microfluidic scanning system to demonstrate the use of graphically encoded gel particles for rapid microRNA quantification (see picture). A versatile particle encoding scheme allows for scalable multiplexing that provides attomole sensitivity with a simple and efficient workflow.



Bioanalytical Methods

S. C. Chapin, D. C. Appleyard, D. C. Pregibon, P. S. Doyle* — 2289–2293

Rapid microRNA Profiling on Encoded Gel Microparticles

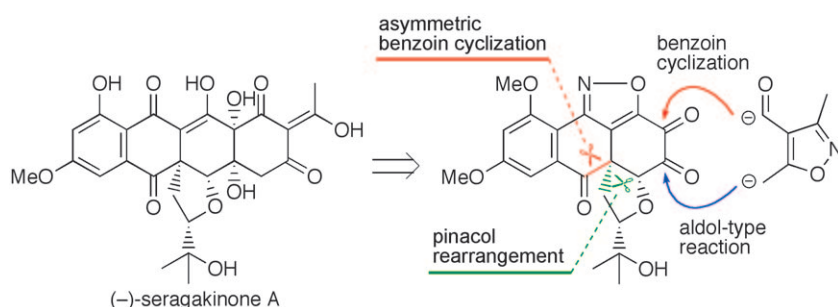


Through the pore: The N-terminal domain of the lethal factor of anthrax toxin was modified to probe protein translocation through the toxin pore. Replacing acidic residues with cysteine acid inhibited translocation, whereas introduction of D-amino acids or an alternating Lys–Glu sequence had no effect. The findings demonstrate independence of translocation from stereospecificity and strict sequence, and dependence on the charge state of acidic residues.

Protein Translocation

B. L. Pentelute, O. Sharma, R. J. Collier* — 2294–2296

Chemical Dissection of Protein Translocation through the Anthrax Toxin Pore



Cyclic transformation: The key transformations of the asymmetric total synthesis of the marine-derived natural product seragakinone A are two N-heterocyclic

carbene catalyzed benzoil cyclizations that result in the construction of two rings and a pinacol-type rearrangement to install the angular prenyl substituent.

Natural Product Synthesis

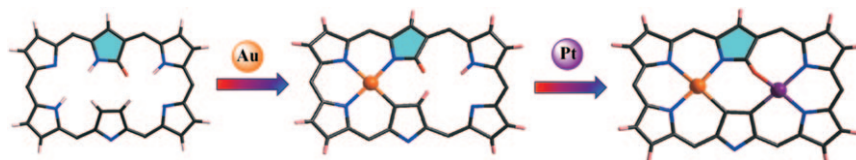
A. Takada, Y. Hashimoto, H. Takikawa, K. Hikita, K. Suzuki* — 2297–2301

Total Synthesis and Absolute Stereochemistry of Seragakinone A



Porphyrinoids

S. Gokulnath, K. Yamaguchi, M. Toganoh, S. Mori, H. Uno, H. Furuta* **2302–2306**



Singly N-Confused [26]Hexaphyrin: A Binucleating Porphyrinoid Ligand for Mixed Metals in Different Oxidation States

Mix and match: The title porphyrinoid has been synthesized and shows unique coordination chemistry by incorporating two different metals with different oxida-

tion states (see figure). X-ray crystallography was used to confirm that a rectangular conformation in both mono- and binuclear complexes was retained.

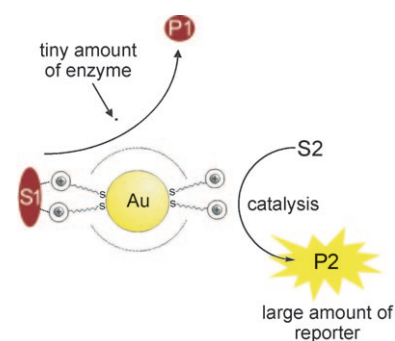
Enzyme Assays

R. Bonomi, A. Cazzolaro, A. Sansone, P. Scrimin,* L. J. Prins* **2307–2312**



Detection of Enzyme Activity through Catalytic Signal Amplification with Functionalized Gold Nanoparticles

A cascade of two catalytic events was used to detect enzyme activity: When a peptide substrate acting as an inhibitor for a catalytic gold nanoparticle was hydrolyzed by an enzyme, the catalytic activity of the nanoparticle was restored, and a large amount of a yellow reporter molecule was produced (see picture; S = substrate, P = product). The assay can be made selective for a particular enzyme by changing the inhibitory peptide.

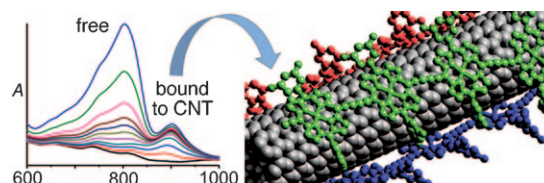


Carbon Nanotubes

J. K. Sprafke, S. D. Stranks, J. H. Warner, R. J. Nicholas, H. L. Anderson* **2313–2316**



Noncovalent Binding of Carbon Nanotubes by Porphyrin Oligomers



Like the tentacles of an octopus: Porphyrin oligomers bind strongly to single-walled carbon nanotubes, and debundle multitube aggregates. The strength of this interaction increases sharply with the number of porphyrin units in the oligo-

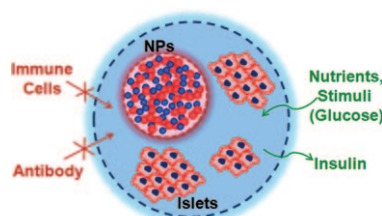
mer, and the affinity is greatest for chiral (7,5) and (8,6) tubes. Quantitative information on these noncovalent recognition processes was obtained from UV/Vis/NIR absorption (see picture) and fluorescence titrations.

Cell Delivery

J. Kim, D. R. Arifin, N. Muja, T. Kim, A. A. Gilad, H. Kim, A. Arepally, T. Hyeon,* J. W. M. Bulte* **2317–2321**



Multifunctional Capsule-in-Capsules for Immunoprotection and Trimodal Imaging

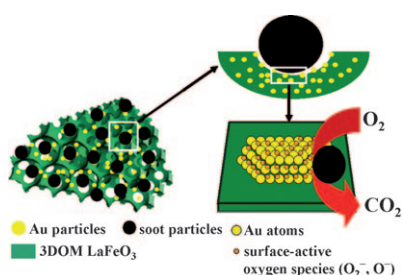


The separate encapsulation of nanoparticles (NPs) and pancreatic islets in an alginate capsule-in-capsule (CIC) structure prevents the nanoparticles being toxic to the cells while housing a high payload of nanoparticles for imaging purposes (see picture). The CIC-encapsulated islets showed an improved insulin secretion over cells encapsulated in single capsules and their transplantation into diabetic mice restored normal glycemia.

pounds were characterized by single-crystal X-ray studies and by solution and solid-state NMR spectroscopy. DFT calculations elucidated the bonding situation.

S. S. Sen, S. Khan, H. W. Roesky,*
D. Kratzert, K. Meindl, J. Henn, D. Stalke,*
J.-P. Demers, A. Lange — **2322–2325**

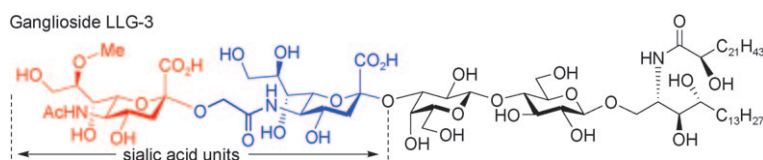
Zwitterionic $\overline{\text{Si-C-Si-P}}$ and $\overline{\text{Si-P-Si-P}}$ Four-Membered Rings with Two-Coordinate Phosphorus Atoms



The catalyst support 3DOM LaFeO₃ contains highly ordered macropores that are connected with each other by small windows. 3DOM LaFeO₃ supported gold catalysts, which combine the advantages of good contact by the macroporous support and highly active sites for activation of O₂ by gold clusters, exhibit super catalytic performance for soot oxidation.

Y. Wei, J. Liu,* Z. Zhao,* Y. Chen, C. Xu,
A. Duan, G. Jiang, H. He — **2326–2329**

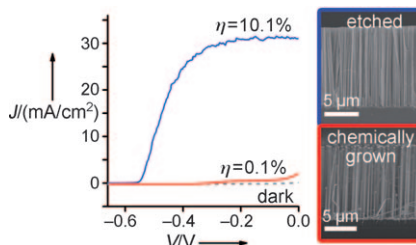
Highly Active Catalysts of Gold Nanoparticles Supported on Three-Dimensionally Ordered Macroporous LaFeO_3 for Soot Oxidation



precursor. The potentially difficult conjugation of the phytoceramide portion with the glycan portion was achieved through the glucosyl ceramide cassette approach.

H. Tamai, H. Ando,* H.-N. Tanaka,
R. Hosoda-Yabe, T. Yabe, H. Ishida,
M. Kiso* _____ **2330–2333**

The Total Synthesis of the Neurogenic Ganglioside LLG-3 Isolated from the Starfish *Linckia laevigata*



G. Yuan, K. Aruda, S. Zhou, A. Levine,
J. Xie, D. Wang* _____ **2334–2338**

Understanding the Origin of the Low Performance of Chemically Grown Silicon Nanowires for Solar Energy Conversion

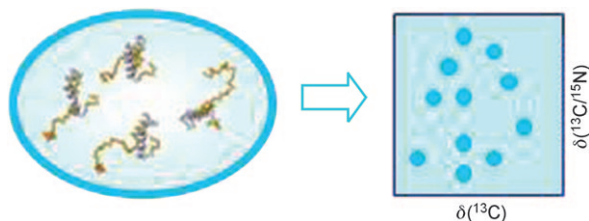


In-Cell NMR Spectroscopy

I. Bertini,* I. C. Felli, L. Gonnelli,
V. Kumar M. V., R. Pierattelli **2339–2341**



¹³C Direct-Detection Biomolecular NMR
Spectroscopy in Living Cells



A direct response: Exclusively heteronuclear ¹³C direct-detection 2D NMR experiments are performed on ¹³C,¹⁵N-enriched proteins in *E. coli* cells. Unfolded proteins or protein fragments provide well-

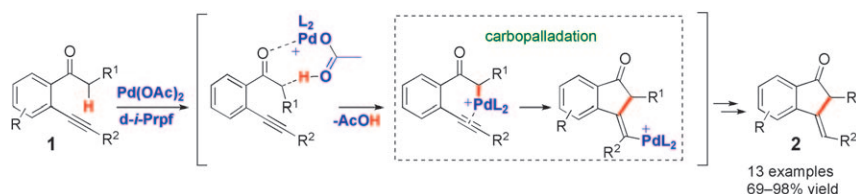
resolved carbonyl detection (see picture), whereas folded proteins or structured motifs do not give any detectable spectrum.

C–H Functionalization

N. Chernyak, S. I. Gorelsky,*
V. Gevorgyan* **2342–2345**



Palladium-Catalyzed Carbocyclization of
Alkynyl Ketones Proceeding through a
Carbopalladation Pathway



Dig this: 5-*exo*-dig carbocyclization of **1** into **2** features intramolecular carbopalladation of alkyne with Pd enolate (see scheme). DFT calculations show that the key Pd enolate forms by deprotonation

assisted by Pd^{II} acetate. Subsequent intramolecular alkyne carbopalladation, *Z*–*E* isomerization of the formed vinyl palladium species, and protodepalladation leads to *E*-alkylidene indanones.

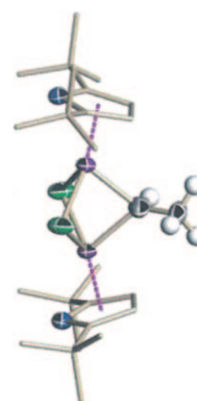
Catalyst Design

S. Licciulli, K. Albahily, V. Fomitcheva,
I. Korobkov, S. Gambarotta,*
R. Duchateau* **2346–2349**



A Chromium Ethylidene Complex as a
Potent Catalyst for Selective Ethylene
Trimerization

Going one, twice... Reaction of the mononuclear complex $[\{\eta^5\text{-}(t\text{Bu})_2\text{C}_4\text{H}_2\text{N}\}\text{CrCl}_2(\text{thf})]$ with AlEt_3 afforded the dinuclear species $[\{\{\eta^5\text{-}(t\text{Bu})_2\text{C}_4\text{H}_2\text{N}\}\text{CrEt}\}_2(\mu\text{-Cl})_2]$ (see picture; Cr purple, Cl green, C sticks/gray, H white). The complex acts as a single-component selective trimerization catalyst; a higher loading of AlEt_3 activator afforded isomerization of 1-hexene to *cis*, *trans* 2-hexene.

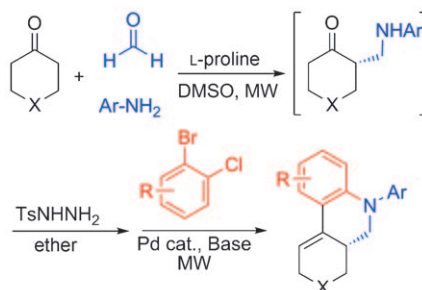


Tandem Catalysis

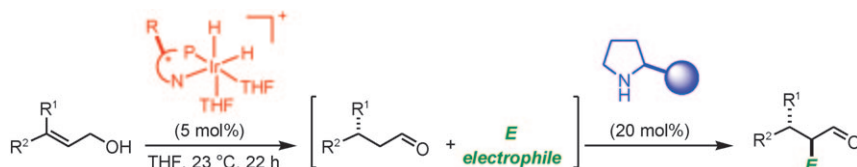
J. Barluenga,* N. Quiñones, M. P. Cabal,
F. Aznar, C. Valdés* **2350–2353**



Tosylhydrazide-Promoted Palladium-
Catalyzed Reaction of β-Aminoketones
with *o*-Dihaloarenes: Combining
Organocatalysis and Transition-Metal
Catalysis



Working in tandem: Mannich adducts obtained by organocatalyzed processes are readily transformed into phenanthridine and quinoline derivatives by a Pd-catalyzed cascade reaction involving tosylhydrazide (TsNHNH_2)-promoted cross-coupling followed by intramolecular amination (see scheme; MW = microwave). The enantioselectivity achieved in the organocatalytic reaction is maintained throughout the process.



Independent workers with team spirit: A catalytic sequence that exploits the compatibility of (chiral) cationic iridium catalysts for the isomerization of primary allylic alcohols to aldehydes with organo-

highly enantioselective α functionalization of aldehydes (see scheme: up to 66 % yield, d.r. 49:1, 99 % ee). The reaction displayed useful generality with respect to both the nucleophile and the electrophile.

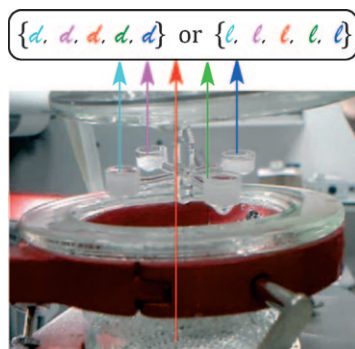
Sequential Catalysis

A. Quintard, A. Alexakis,*
C. Mazet* ————— 2354–2358

Access to High Levels of Molecular Complexity by One-Pot Iridium/Enamine Asymmetric Catalysis



This way or that: Analysis of the chiral composition of the crystal mixture obtained from samples of boiling solutions of NaClO₃ (see picture) indicates that symmetry breaking towards homo-chiral compositions may begin in the metastable stage preceding crystallization, that is, at the level of subcritical clusters.



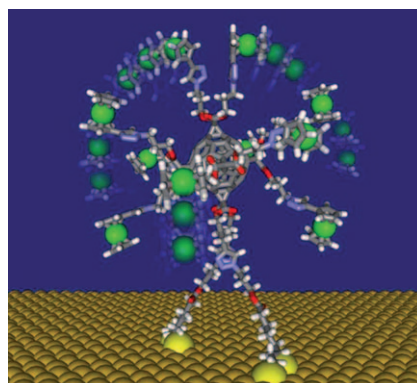
Chirality

Z. El-Hachemi,* J. Crusats, J. M. Ribó,*
J. M. McBride,
S. Veintemillas-Verdaguer* — 2359–2363

Metastability in Supersaturated Solution and Transition towards Chirality in the Crystallization of NaClO₃



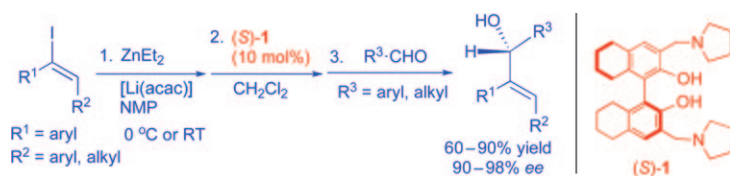
A rigid 3D scaffold in a 2D world! A mixed [5:1] fullerene hexaadduct that bears ten peripheral ferrocene redox subunits has been anchored onto a gold surface (see picture, green: iron, black: carbon, white: hydrogen, red: oxygen, blue: nitrogen). Ultrafast cyclic voltammetry investigations revealed that both intramolecular electron hopping and molecular motions influence the electron transfer from the ferrocene moieties to the electrode.



Electron Transfer

P. Fortgang, E. Maisonhaute,*
C. Amatore,* B. Delavaux-Nicot,* J. Lehl,
J.-F. Nierengarten* ————— 2364–2367

Molecular Motion Inside an Adsorbed [5:1] Fullerene Hexaadduct Observed by Ultrafast Cyclic Voltammetry



Mild and tolerant: Vinylzinc reagents were directly prepared from the reaction of vinyl iodides with ZnEt₂ under mild reaction conditions. The compound (S)-1 was found to catalyze the addition of the vinylzinc reagents to a variety of aldehydes to generate structurally diverse allylic

alcohols with high yields and enantioselectivities. This catalytic process can tolerate functional groups such as esters, chlorine, ethers, and silyl ethers on the substrates. acac = acetylacetonate, NMP = *N*-methyl-2-pyrrolidone.

Asymmetric Catalysis

A. M. DeBerardinis, M. Turlington,
L. Pu* ————— 2368–2370

Activation of Vinyl Iodides for the Highly Enantioselective Addition to Aldehydes



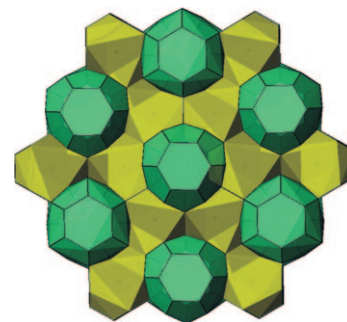
Clathrates

M. A. Kirsanova, A. V. Olenov,
A. M. Abakumov, M. A. Bykov,
A. V. Shevelkov* ————— **2371 – 2374**



Extension of the Clathrate Family: The
Type X Clathrate $\text{Ge}_{79}\text{P}_{29}\text{S}_{18}\text{Te}_6$

Now they are 10! The title compound displays a new type of crystal structure and is labeled clathrate X according to the general classification of clathrate structures. In contrast to typical clathrates, this compound has three-coordinate atoms within the framework and combines distorted 24-vertex polyhedra (see picture, green) centered around tellurium guest atoms with very irregular 10-vertex polyhedra around sulfur atoms (yellow).

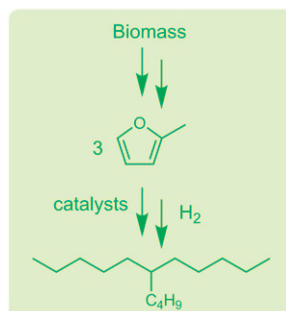


Sustainable Chemistry

A. Corma,* O. d. I. . Torre, M. Renz,
N. Vollandier ————— **2375 – 2378**



Production of High-Quality Diesel from
Biomass Waste Products



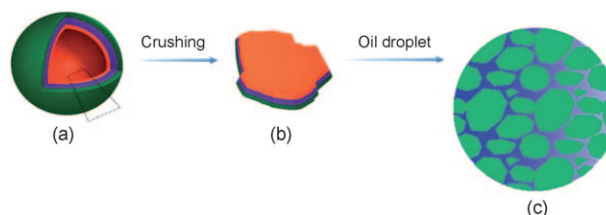
High-quality liquid fuels are obtained from non-edible carbohydrates by energy-efficient processes. 2-Methylfuran, produced by hydrogenation of furfural, is converted into 6-alkyl undecanes in a catalytic solvent-free process (see scheme with 6-butylundecane). A diesel fuel is produced with an excellent motor cetane number (71) and pour point (-90°C) and with global process conversions and selectivities close to 90%.

Janus Particles

F. X. Liang, K. Shen, X. Z. Qu, C. L. Zhang,
Q. Wang, J. L. Li, J. G. Liu,
Z. Z. Yang* ————— **2379 – 2382**



Inorganic Janus Nanosheets



Another face to Janus particles: Silica Janus nanosheets were synthesized by crushing Janus hollow spheres formed by self-assembled materialization of an

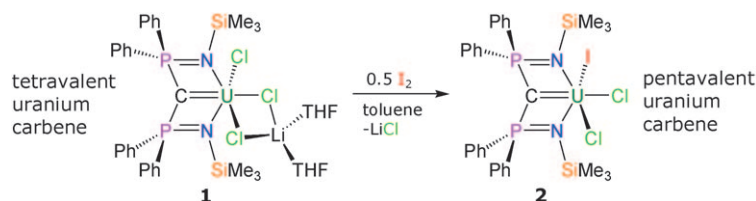
amphiphilic emulsion interface. The Janus nanosheets serve as solid surfactants and can be used collecting oil or hazardous chemical spills.

Uranium Carbene Complexes

O. J. Cooper, D. P. Mills, J. McMaster,
F. Moro, E. S. Davies, W. Lewis, A. J. Blake,
S. T. Liddle* ————— **2383 – 2386**

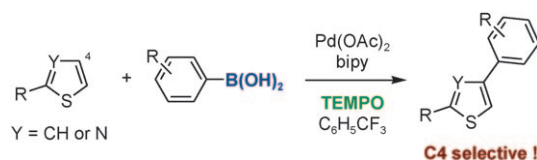


Uranium–Carbon Multiple Bonding:
Facile Access to the Pentavalent Uranium
Carbene $[\text{U}\{\text{C}(\text{PPh}_2\text{NSiMe}_3)_2\}(\text{Cl})_2(\text{I})]$ and
Comparison of $\text{U}^{\text{V}}=\text{C}$ and $\text{U}^{\text{IV}}=\text{C}$ Bonds



A straightforward oxidation strategy affords the first pentavalent uranium carbene complex, **2**. Owing to the structural similarity of **1** and **2**, it was possible

for the first time to directly probe the differences in $\text{U}=\text{C}$ bonding on oxidation of U^{IV} to U^{V} .



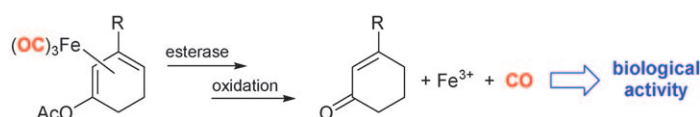
It adds up to 4! Thiophenes and thiazoles can be arylated in the 4- rather than the expected 5-position in a new C–H functionalization reaction (see scheme; TEMPO: 2,2,6,6-tetramethylpiperidine-N-oxyl). The boronic acid proved to be the

key to achieving the otherwise difficult C4 selectivity. The method was applied to a concise synthesis of a key pharmacological structure with potential for treatment of Alzheimer's disease.

Oxidative C–H Arylation

S. Kirchberg, S. Tani, K. Ueda,
J. Yamaguchi, A. Studer,*
K. Itami* _____ **2387 – 2391**

Oxidative Biaryl Coupling of Thiophenes and Thiazoles with Arylboronic Acids through Palladium Catalysis: Otherwise Difficult C4-Selective C–H Arylation Enabled by Boronic Acids



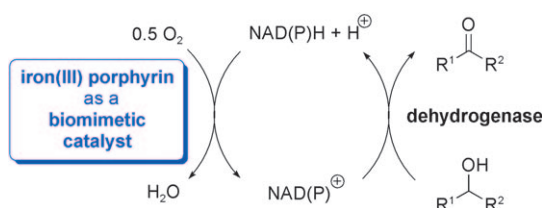
Molecular hazardous materials transport: Enzyme-triggered CO-releasing molecules (ET-CORMs) offer new options for the delivery of CO. The cleavage of dienylester iron tricarbonyl complexes by an esterase

under mild oxidative conditions generates CO, which causes a strong inhibiting activity of the compounds to inducible nitric oxide synthase as shown in a cellular assay.

Carbon Monoxide Release

S. Romanski, B. Kraus,
U. Schatzschneider, J.-M. Neudörfl,
S. Amslinger,*
H.-G. Schmalz* _____ **2392 – 2396**

Acyloxybutadiene Iron Tricarbonyl Complexes as Enzyme-Triggered CO-Releasing Molecules (ET-CORMs)



An enzyme substitute: A synthetic Fe^{III} porphyrin was used as a catalyst for the activation and reduction of O₂ into H₂O with the cofactor NAD(P)H in aqueous solution. The catalyst is compatible with different preparative enzymatic oxidation

reactions. Thus, a new method is provided for the in situ regeneration of the oxidized cofactor NAD(P)⁺ with help from a non-enzymatic, synthetic catalyst (see scheme).

Metalloporphyrins

H. Maid, P. Böhm, S. M. Huber, W. Bauer,
W. Hummel, D. N. Jux,
H. Gröger* _____ **2397 – 2400**

Iron Catalysis for In Situ Regeneration of Oxidized Cofactors by Activation and Reduction of Molecular Oxygen: A Synthetic Metalloporphyrin as a Biomimetic NAD(P)H Oxidase

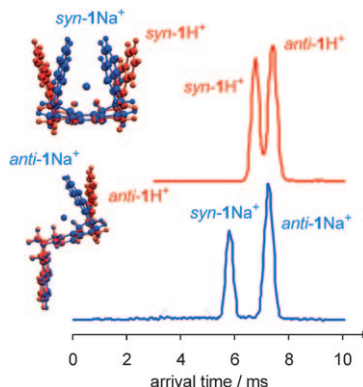


Ion-Mobility Mass Spectrometry

Á. Révész, D. Schröder,* T. A. Rokob,
M. Havlík, B. Dolenský — 2401–2404



In-Flight Epimerization of a Bis-Tröger Base



Increased mobility is observed for the sodiated *syn* and *anti* isomers of bis-Tröger base **1** relative to that of the protonated variants. Ion-mobility measurements further demonstrate that the pseudo-epimerization of the bis-Tröger base proceeds by a proton-mediated ring opening rather than a retro-Diels–Alder sequence.



Supporting information is available on www.angewandte.org (see article for access details).



A video clip is available as Supporting Information on www.angewandte.org (see article for access details).



This article is available online free of charge (Open Access)

Sources

Product and Company Directory

You can start the entry for your company in “Sources” in any issue of *Angewandte Chemie*.
If you would like more information, please do not hesitate to contact us.

Wiley-VCH Verlag – Advertising Department

Tel.: +49 62 01 - 60 65 65

Fax: +49 62 01 - 60 65 50

E-Mail: MSchulz@wiley-vch.de

Service

Spotlight on Angewandte's Sister Journals — 2208–2210

Preview — 2405

The issues for February 2011 appeared online on the following dates
Issue 5: January 26 • Issue 6: February 2 • Issue 7: February 9 • Issue 8: February 16 • Issue 9: February 22

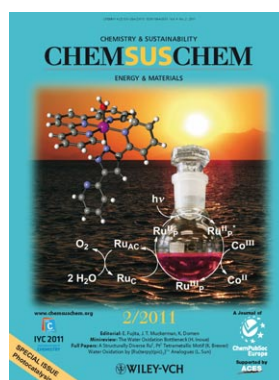
Check out these journals:



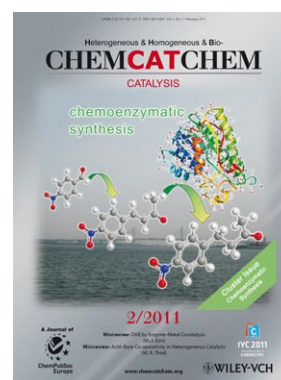
www.chemasianj.org



www.chemmedchem.org



www.chemsuschem.org



www.chemcatchem.org